

THERMAL CONDUCTIVITY AND WEAR RESISTANCE OF A359/(SiC + Si₃N₄) HYBRID COMPOSITES PREPARED BY SQUEEZE CASTING

E. A. M. Shalaby,^{1,3} A. Churyumov,¹ M. Abou El-Khairb,² and A. Daoud²

Translated from *Novye Ogneupory*, No. 4, pp. 116 – 123, April, 2018.

Original article submitted December 26, 2017.

Thermal parameters and wear are considered with dry sliding for hybrid composites based on an A359 matrix prepared by squeeze casting. Composites are strengthened with addition of 5, 10, and 15 wt.% (SiC + Si₃N₄). Wear of A359/(SiC + Si₃N₄) composites proceeds under a load in the range 20 – 60 N with a sliding rate of 2.75 m/sec. It is found that A359/(SiC + Si₃N₄) composite exhibits relatively low thermal conductivity and better wear resistance than alloy A359. Friction coefficients and surface contact temperature for specimens of composite A359/(SiC + Si₃N₄) increase as there is an increase in (SiC + Si₃N₄) content within them. In studying worn surfaces it is detected that A359/(SiC + Si₃N₄) composite is covered with iron oxide that plays the role of a self-lubricating layer. The better wear resistance index for A359/(SiC + Si₃N₄) composites makes it possible to use them in the automobile industry.

Keywords: dry strengthening addition, thermal conductivity, wear, friction coefficient.

INTRODUCTION

Development of strong lightweight materials is of interest for the automobile industry. The main aim of using lightweight materials includes a reduction in fuel requirements and also as a consequence saving energy and reducing greenhouse gases. In order to produce these materials composites with a matrix of aluminum metal (AMMCs) are promising since they exhibit mechanical and tribological strength compared with normal aluminum alloys. Therefore, their splendid properties are used in aerospace and automobile industries [1 – 9]. With dry friction such forged materials as aluminum alloys normally demonstrate significant wear [10 – 19]. During AMMCs production various strengthening additions are made to their composition in order to increase wear resistance and improve mechanical properties [20 – 23]. It is noted that the wear resistance of Al–Si alloys is also affected by such production factors as loading, rate, lubrication, surface morphology, microstructure, and volume fraction of silica [24 – 28]. Natarazhan and others [19] point to significant improvement of the wear resistance of

A356/125% SiC composite under action of dry friction. Also well known is the reduction in wear rate for Al?Si alloy with addition of 15 – 20 wt.% SiC [29]. A considerable part of the research of wear of AMMCs composites has been performed using iron contact surfaces (ferrous counterfaces). Significant binding reaction is observed between AMMCs and ferrous materials that is seen in the formation in the course of wear of a layer at an AMMCs surface [6, 8]. In addition, wear characteristics for composites under similar conditions are more favorable than with annealing or use of unstrengthened alloy [30 – 32]. In order to strengthen AMMCs composites there is extensive use of SiC ceramic particles since they exhibit good strength and resistance to mechanical action, significant wear resistance, and corrosion resistance, low LTEC, and also low cost [33 – 36].

On the other hand Si₃N₄-ceramic exhibits high strength and wear resistance. In addition it has low density and LTEC. Due to the splendid mechanical properties of this ceramic it may be used for example in producing pistons, brake rotors, and drums, and also refractories. There is information [37 – 39] about of loose Si₃N₄-ceramic, its behavior during wetting, mechanical properties and microstructure. It may be confirmed that AMMCs/Si₃N₄ composites may be used in very different areas.

¹ FGAOU VO NITU MISiS, Moscow, Russia.

² Central Metallurgical Scientific-Research Institute, Cairo, Egypt.

³ eshelaby2000@yahoo.com

Currently AMMCs composites are prepared by a solid-phase or liquid-phase method [40, 41]. However, due to the clear advantage of production by a liquid phase method the greatest part of AMMCs composites used in industry is in fact produced by this technology. In addition, liquid metal technology of less expensive. It is simpler to operate with liquid metal than with powder. It is possible to prepare composites of different shapes from liquid metal [42]. During AMMCs production there is extensive use of mixing [32, 43]. Composites prepared by mixing technology exhibit greater porosity than composites prepared by squeeze casting [43]. Squeeze casting has a favorable effect on solidification time, and compaction in a permanent mold and forging makes it possible to increase wear resistance and to improve the composite mechanical properties, and also to strengthen the phase interface due to a reduction in porosity between matrix alloy and strengthening additives, as a result of which more reliable mechanical adhesion is obtained [44].

The authors of present work have introduced different amounts of SiC and Si₃N₄ into matrix alloy A359 as strengthening from mixtures of their particles and with use of squeeze casting. The effect of additions on thermal conductivity, wear resistance, and friction resistance with different loads has been studied.

EXPERIMENTAL METHOD

Composite treatment

The matrix alloy A359 used was of the following composition, wt. %: 9.1 Si, 0.58 Mg, balance Al. SiC and Si₃N₄ particles were added in the form of strengthening particles to alloy A359 in an amount of 5, 10, and 15 wt. % in accordance with the ratio 2:1. The grain size composition of the additive was correspondingly 40 and 3 μm. At first composites were prepared by mixing technology, and then by squeeze casting. Alloy A359 was melted at 1350°C. In order to remove impurities from the let surface layer was collected before introducing strengthening additives. The frequency of melt rotation gradually increased as there was an increase in rotation frequency of a titanium stirrer to 850 rpm. This was required in order to create turbulence during introduction of additives. Mixing lasted for 1 min after introduction of dry substances in order to guarantee uniform distribution of additions to the matrix. Then composites atomized at 680°C were placed in a previously heated (200°C) steel mold in the form of a cylinder with an inner diameter of 50 mm. The temperature of the plunger and piston was 200°C and the pressure was 100 MPa. Holding duration in the course melt compaction was 1 min; then solidified specimens were extracted from the mold.

Measurement of thermal conductivity

Cylindrical disks 2.7 mm in diameter and 2 mm thick were prepared from A359 composites. Thermal conductivity

of specimens in the form of disks was determined in an LFA (Netzsch) instrument for performing thermal analysis. An average value was obtained from measurements for four specimens. Specific heat content was A359 specimens was measured in a Setaram Labsys differential scanning calorimeter in argon in the range 25 – 300°C, and density was determined by Archimedes rule Composite thermal conductivity was evaluated by an equation

$$\lambda = c_p \rho \alpha,$$

where λ is thermal conductivity, c_p is specific heat content; ρ is density; α is thermal conductivity.

Wear measurement

Tests were conducted in an instrument for testing friction and wear by a pin and disc scheme. In this case pins of composite 8 mm in diameter and 11 mm long slid over a rotating steel disk 200 mm in diameter and 3 mm thick, and with hardness HRC 62. A Surfest SJ-201P instrument was used in order to measure roughness R_a ; R_a of control specimens and a steel disk before testing was correspondingly 1.55 and 0.35 μm. The track radius was maintained at a constant level (42 mm) and the disk rotation frequency 655 rpm, which provided a constant sliding rate of 2.75 m/sec. Applied test loads were increased from 20 to 60 N, which corresponded to load levels of 0.40 and 1.19 MPa. Sliding tests were performed continuously for 30 min. Temperature at the start of a test was 20°C. After several minutes the track was contaminated with wear particles. The temperature of the pin surface and force of friction was recorded for each 5 min. Temperature was recorded with an accuracy of 0.1 °C, and friction force with precision of 0.1 N. Data were used to determine friction coefficient. By means of electronic scales with sensitivity of 0.0001 g pin specimen weight loss was evaluated. The wear rate if a pin R , mm³/m, was determined by an equation [20]

$$R = \frac{\Delta W}{d\rho},$$

where ΔW is weight loss; d is sliding distance.

After completion of a test worn pin surfaces were studied in a Vega 3 LMH (Tescan) scanning electron microscope (SEM). Surface morphology and chemical composition of wear particles were studied using and energy-dissipation analyzer (EDXA).

RESULTS AND DISCUSSION

Thermal conductivity

The dependence of A359/(SiC + Si₃N₄) thermal conductivity with a different amount of additive is shown in Fig. 1. It was detected that the thermal conductivity of an

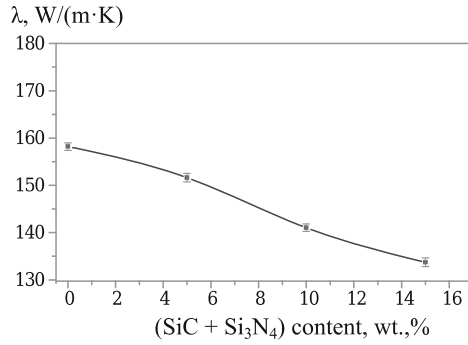


Fig. 1. Effect of amount of (SiC + Si₃N₄) strengthening phase on composite λ.

A359/(SiC + Si₃N₄) composite decreases linearly from 158.2 to 130.7 W/(m·K) as there is an increase in the amount of (SiC + Si₃N₄) to 15%. This feature is explained by the difference in the thermal conductivity of (SiC + Si₃N₄) particles and matrix alloy A359. However, it should be noted that the form of loose additive, its amount, apparent density, and porosity, and also treatment technology, are significant factors affecting composite thermal conductivity [24, 25].

Use of squeeze casting technology plays an important role in increasing the thermal conductivity of A359/(SiC + Si₃N₄) composite, guaranteeing preparation of strong composites with low porosity and high density. Therefore, dense contact between components of a composite improves its thermal conductivity. In addition, the thermal conductivity of a A359/5 wt.% (SiC + Si₃N₄) composite is 151.62 W/(m·K) with porosity of 0.85%, and for a composite A359/15 wt.%(SiC + Si₃N₄) it is 130.72 W/(m·K) with porosity of 1.95%. This signifies that a reduction in composite A359/(SiC + Si₃N₄) thermal conductivity proceeds as a result of a change in porosity. Therefore, the amount of strengthening additive and porosity have a strong effect on composite A359 thermal conductivity.

The change in composite A359/(SiC + Si₃N₄) thermal conductivity in relation to temperature is shown in Fig. 2. As there is an increase in temperature thermal conductivity gradually decreases. However, thermal conductivity is affected not only by temperature, but also the form of strengthening additive and also its composition: in the heating range (25 – 300°C) there is a significant reduction in A359/(SiC + Si₃N₄) composite thermal conductivity. In order to determine the thermal conductivity of different materials, including composites with a metal matrix, Maxwell and Eucken [46] proposed a simplified form assuming an ideal bond between loose material and matrix in the composite obtained. In the present work the Maxwell – Eucken equation is used for theoretical evaluation of composite thermal conductivity

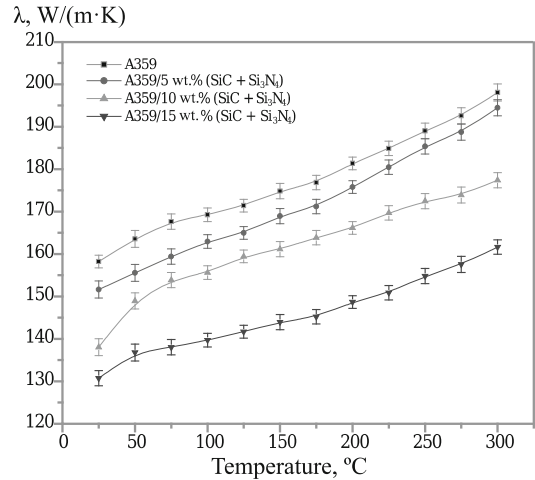


Fig. 2. Dependence of composite λ on temperature.

$$\lambda = \lambda_m \left(\frac{2 \left(\frac{\lambda_p}{\lambda_m} - 1 \right) V_p + \frac{\lambda_p}{\lambda_m} + 2}{\left(1 - \frac{\lambda_p}{\lambda_m} \right) V_p + \frac{\lambda_p}{\lambda_m} + 2} \right)$$

where λ is composite thermal conductivity; λ_p is loose material thermal conductivity (in this study it is 77 and 35 W/(m·K) for SiC and Si₃N₄ respectively); λ_m is alloy A350 thermal conductivity (161 W/(m·K)); V_p is volume fraction of added particles.

Comparison of experimental and theoretical values of A359 composite thermal conductivity with a different content of strengthening additives is provided below:

Composite	A359 (matrix)	C 5 wt.% (SiC + Si ₃ N ₄)	C 10 wt.% (SiC + Si ₃ N ₄)	C 15 wt.% (SiC + Si ₃ N ₄)
Thermal conductivity, W/(m·K):				
theoretical	161.00	152.62	144.53	136.72
experimental	158.20	148.62	138.03	130.72

As is seen, experimental results almost coincide with those calculated the Maxwell–Eucken equation, which confirms the strong connection between ceramic loose material and a matrix of alloy A359. This especially concerns a A359/(SiC + Si₃N₄) composite. In addition, this confirms presence of small or insignificant damage around additive particles. Therefore, use of pressure during employment of squeeze casting technology may be considered as valid. In addition, important factors should also be considered such as matrix alloy grade, type and grain size of composition of loose additive [24, 37 – 39].

Two types of particles (SiC + Si₃N₄) have been used in the present work with different grain size composition. Finer particles of Si₃N₄ and intended for improving mechanical properties, and the relatively coarser particles of SiC are intended for increasing wear resistance. The additive grain size composition not only affects composite thermal conductivity,

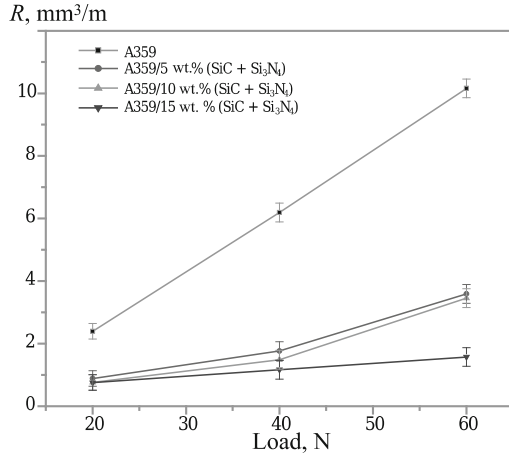


Fig. 3. Effect of load on composite wear rate R .

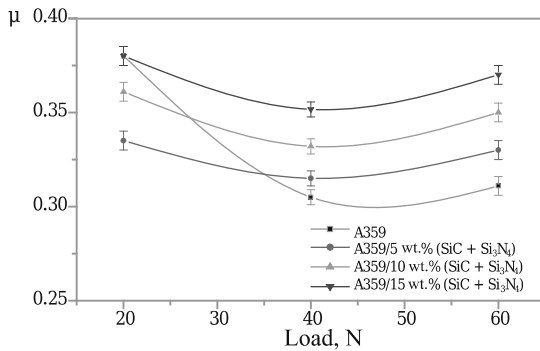


Fig. 4. Dependence of composite friction coefficient μ on load.

but also facilitates an increase in wear resistance. It has been established that additive with a coarser grain size (as in this study) will be fastened with the matrix during a longer time than additive with a finer grain size.

Dependence of wear rate on load

The effect of load on A359/(SiC + Si₃N₄) composite wear rate is shown in Fig. 3. As is seen, composites demonstrate significantly better wear resistance than alloy A359. A matrix of A359 is a material subject to maximum wear rate with all of the loads used. Wear rate decreases with all loads as there is an increase in amount of strengthening additive (SiC + Si₃N₄). With a load of 20 N the A359/(SiC + Si₃N₄) composite wear rate is a little lower than for alloy A359, but with a load of 60 N it is significantly lower than for alloy A359, i.e., the differences between wear rates for composites and A359 matrix is very marked.

In addition, the wear rate for a composite based on A359 is considerably reduced as there is an increase in amount of strengthening additive. A possible explanation for this includes the following: as there is an increase in additive content there is an increase in surface area between additive and a steel disk, and additive hinders direct participation of ma-

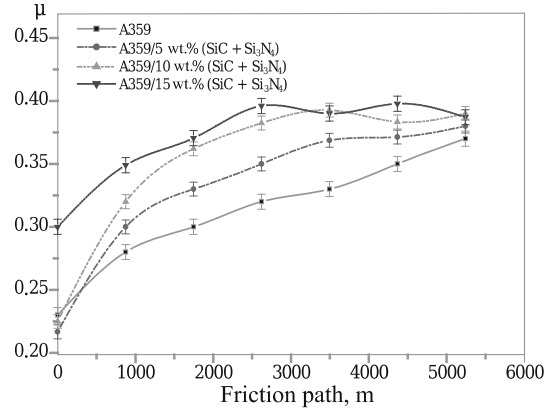


Fig. 5. Dependence of composite μ on friction path.

trix in the wear process. If the amount of additive large, it covers a whole specimen surface. Therefore, the contact area is only between additive and a steel disk. As a consequence, an increase in (SiC + Si₃N₄) content in composites based on A359 reduces wear rate. In addition, with relatively high loads (60 N) for A359/(SiC + Si₃N₄) composites there is a slower wear rate than for the A359 matrix. This occurs due to the enormous superiority of ceramic material (SiC + Si₃N₄) particle properties; low LTEC, significant strength splendid hardness and wear resistance [37 – 39] The superb metallic properties of ceramic material (SiC + Si₃N₄) and its wear resistance facilitate a reduction in wear rate.

Effect of load and friction path on friction coefficient

The friction coefficient μ for A359/(SiC + Si₃N₄) composite increases as there is an increase in load in the range 20 – 60 N (Fig. 4). Normally μ for composites and the A359 matrix increases with an increase in load from 20 to 60 N, and for A359/(SiC + Si₃N₄) composites it is higher than for an alloy A359 matrix with an identical load. This is explained by the significant action of (SiC + Si₃N₄) material high hardness, due to which greater friction forces arise in the course of the wear process.

The change in friction coefficient is shown in Fig. 5 in relation to friction path with a load of 60 N for a matrix of A359 and a A359/(SiC + Si₃N₄) composite. It is seen that values of friction coefficient increase in the course of movement with sliding. A logical explanation suggests itself: in the course of wear the formation of products in the form of powder, which enters into contact with the friction surface. Then there is an increase in friction area between the two surfaces, which leads to additional wear between wear products and the contact surface. Then plastic deformation of friction increases the amount of deformation strengthening, and as a consequence of this an increase in friction coefficient. On the other hand, Si phases break down and are distributed between composite and the contact surface, which leads to an increase in friction coefficient as there is an increase in friction path.

Increase in composite underlayer temperature in relation to load

The effect of load on the temperature of a A359/(SiC + Si₃N₄) composite underlayer after a friction path of 5241 m is shown in Fig. 6. It is seen that the temperature of the underlayer region increases almost linearly in relation to applied load. A359/(SiC + Si₃N₄) composites demonstrate higher underlayer temperature than the matrix alloy A359. This is explained by the greater friction forces for a A359/(SiC + Si₃N₄) composite during wear. In addition, the greater the amount of SiC in the additive, the higher the underlayer temperature is raised. Due to an increase in contact area and presence of wear products between friction surface the friction force increases and as a consequence there is an increase in surface temperature [47].

Worn surface morphology

SEM microphotographs are shown in Fig. 7 of a worn surface of matrix alloy A359 and A359/(SiC + Si₃N₄) composite tested under a load of 60 N [48]. Presence at the alloy A359 surface (Fig. 7a) of troughs, and cavitation projections in the wear direction point to significant ductility, especially with a load of 60 N. For an A359/(SiC + Si₃N₄) composite in wear surfaces fewer troughs or projections are observed than for alloy A359. This is especially noticeable in Fig. 7c, d for A359/(SiC + Si₃N₄) composites with a higher content of compacting additives. Wear testing is accompanied by plas-

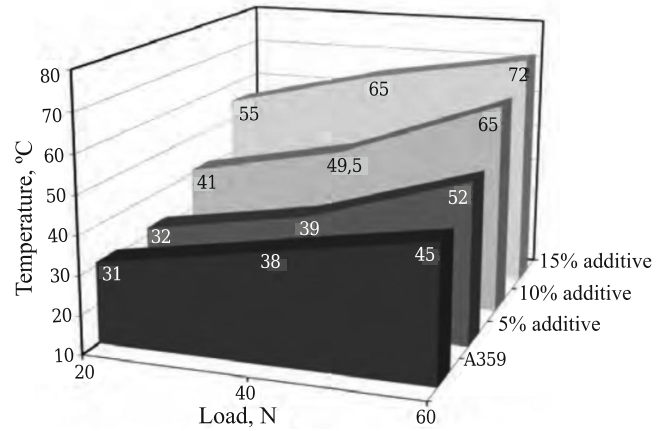


Fig. 6. Effect of load and amount of strengthening additive on composite pin temperature.

tic deformation of a pin surface (see Fig. 7b). This plastic flow of metal in the surface layer of a pin covers (SiC + Si₃N₄) particles and prevents their advance towards the contact surface until a metal layer covering the ceramic material is partly worn away. Then as a result of action of a load a mixture of particles of additive is refined into a finely ground fraction and distributed over the wear surface.

Refined particles are distributed over the pin surface, broken apart and joined forming a continuous film of hard substance (SiC + Si₃N₄) on a worn surface. At the same time,

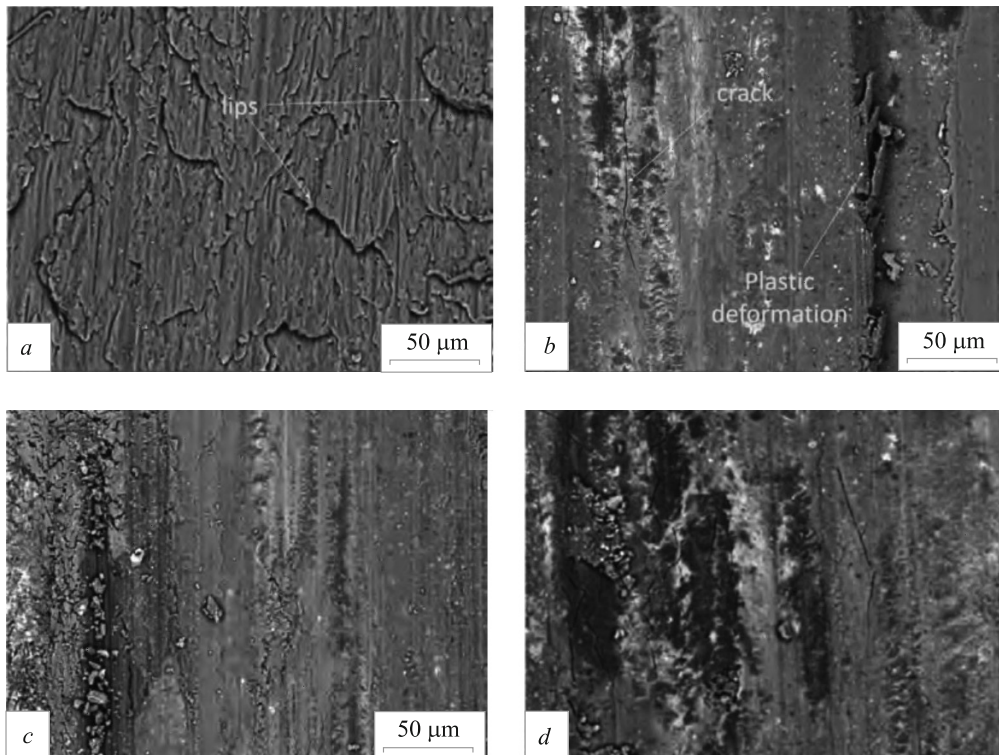


Fig. 7. SEM-microphotographs of A359 composite worn surfaces with a load of 60 N: a) A359 alloy; b) A359/5 wt.% (SiC + Si₃N₄); c) A359/10 wt.% (SiC + Si₃N₄); d) A359/15 wt.% (SiC + Si₃N₄).

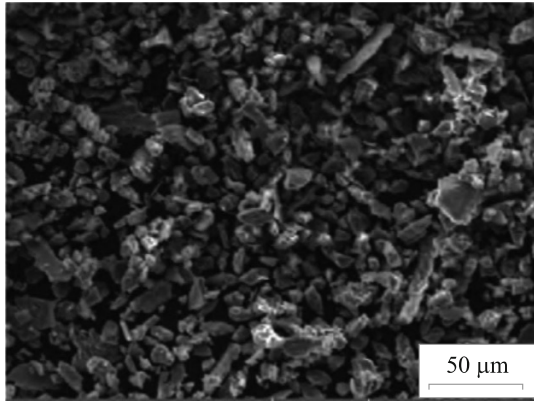


Fig. 8. SEM-microphotographs of A359/15 wt.% (SiC + Si₃N₄) composite wear products tested with a load of 60 N.

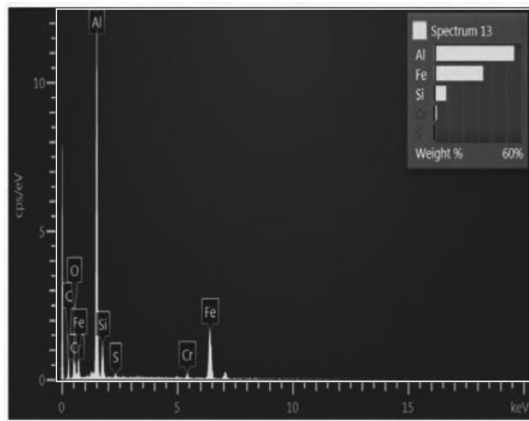


Fig. 9. EDXA-spectrum of A359/15 wt.% (SiC + Si₃N₄) composite wear products tested with a load of 60 N.

a solid hybrid layer develops from broken (SiC + Si₃N₄) particles. As there is wear it spreads at the composite pin surface. Then a film of (SiC + Si₃N₄) is transferred to the contact surface. In the course of this process (SiC + Si₃N₄) material is fed continuously, which acts as a solid layer between the two friction surfaces. That is, the composite becomes more wear resistant due to transfer of ground loose material of additive to the rubbing surfaces and formation on them of a thin film. Therefore, improvement of composite wear characteristics depends on the capacity of (SiC + Si₃N₄) material particles to emerge from the “built-in” position in a matrix and to be distributed uniformly in the form of a solid film between tribological (rubbing) surfaces [20, 47]. This adhesive wear is expressed in the form of adhesive “ploughing” of the pin surface. Wear of A359 depends to a considerable degree on crack generation and propagation over rubbing surfaces. A source of crack generation in Al–Si alloy is the Al/Si interface.

In the initial period of the wear process silicon particles prevent breakdown and protect the surface. Then cracks are

generated, and they join each other forming wear products. Hard silicon particles break into fine lumps separating from the matrix. Crushing of silicon particles proceeds when the load on an Si particles appears to be greater than the silica failure resistance [48]. Worn surfaces of A359/5 wt.% (SiC + Si₃N₄) composites may differ with respect to plastic deformation and short cracks in the sliding direction, These cracks probably arise under the wear surface of the pin, and propagate towards the wear surface. This points to local plastic deformation in the underlayer region, adjacent to a contact surface. Deformation caused by shear leads to occurrence of considerable tension in a worn pin layer. Localization of this tension leads to crack generation and propagation over tracks under action of shear. Considerable plastic deformation normally accelerates generation of cavities and their growth in particles present within underlayer regions. These cavities then join and form a crack and the alloy wear products separate into layers [49].

Wear products of A359/15 wt.% (SiC + Si₃N₄) composite are shown in Fig. 8 under a load of 60 N, having the form of thin platelets and fine particles. They may be considered as wear products over the steel disk and composite pin. The composition of wear products mainly includes Al, Si, Fe, C, O, and Cr (Fig. 9) wear products formed with high loads are a mechanical mixture of particles separating both from specimens and from the contact surface. There are mechanisms of wear product formation including separation at the surface and abrasion. Presence of Fe may be considered as a sign of abrasive action of the projecting ends of (SiC + Si₃N₄) and Si particles on a worn steel contact surface. Broken fragments of ceramic particles are mixed with loose wear products and act as a third abrasive factor, having an effect both on the composite surface, and on the steel surface. Iron oxides, covering wear surfaces, act as a lubricant and provide a smooth form of worn surface finally increasing is wear resistance.

The authors thank the Russian Federation Ministry of Education and Science for financial aid in the framework of Increase Competitiveness Program of NITU MISiS.

REFERENCES

1. A. Daoud and M. T. Abou El-Khair, “Wear and friction behavior of sand cast brake rotor made of A359 – 20 vol. % SiC particle composites sliding against automobile friction material,” *Tribology Int.*, **43**, 544 – 553 (2010).
2. S. Suresh, N. S. V. Moorthi, S. C. Vettivel, et al., “Effect of graphite addition on mechanical behavior of Al6061/TiB₂ hybrid composite using acoustic emission,” *Mater. Sci. Eng. A*, **612**, 16 – 27 (2014).
3. H. Kala, K. K. S. Mer, and S. Kumar, “A review on mechanical and tribological behavior of stir cast aluminum matrix composites,” *Procedia Mater. Sci.*, **6**, 1951 – 1960 (2014).
4. N. C. H. Kaushik and R. N. Rao, “The effect of wear parameters and heat treatment on two body abrasive wear of Al–SiC–Cr hybrid composites,” *Tribology Int.*, **96**, 184 – 190 (2016).

5. G. S. Wang and L. Geng, "Microstructural changes of SiCw/6061Al composite during compression at temperatures below and above the solidus of the matrix alloy," *Mater. Chem. Phys.*, **96**, 2 – 8 (2006).
6. M. Kok "Abrasive wear of Al₂O₃ particle reinforced 2024 aluminium alloy composites fabricated by vortex method," *Composites: Part A*, **37m** 457 – 464 (2006).
7. B. N. Sarada, P. L. Srinivasa Murthy, and G. Ugrasen, "Hardness and wear characteristics of hybrid aluminium metal matrix composites produced by stir casting technique," *Mater. Today: Proceedings*, **2**, 2878 – 2885 (2015).
8. Y. Liu, Z. Han, and H. Cong, "Effects of sliding velocity and normal load on the tribological behavior of a nanocrystalline Al based composite," *Wear*, **268**, 976 – 983 (2010).
9. S. Suresh, N. S. V. Moorthi, N. Vettivel, and S. C. Selvakumar, "Mechanical behavior and wear prediction of stir cast Al–TiB₂ composites using response surface methodology," *Mater. Des.*, **59**, 383 – 396 (2014).
10. J. Liu, J. Binner, and R. Higginson, "Dry sliding wear behaviour of co-continuous ceramic foam / aluminium alloy interpenetrating composites produced by pressureless infiltration," *Wear*, **276/277** 94 – 104 (2012).
11. S. K. Chaudhury, A. K. Singh, C. S. Sivaramakrishnan, and S. C. Panigrahi, "Wear and friction behavior of spray formed and stir cast Al–2Mg–11TiO₂ composites," *Wear*, **258**, 759 – 767 (2005).
12. Y. Wang, W. M. Rainforth, H. Jones, and M. Lieblich, "Dry wear behaviour and its relation to microstructure of novel 6092 aluminium alloy–Ni₃Al powder metallurgy composite," *Wear*, **251**, 1421 – 1432 (2001).
13. J. C. Walker, W. M. Rainforth, and H. Jones, "Lubricated sliding wear behaviour of aluminium alloy composites," *Wear* **259**, 577 – 589 (2005).
14. A. Daoud, "Wear performance of 2014 Al alloy reinforced with continuous carbon fibers manufactured by gas pressure infiltration," *Mater. Lett.*, **58**, 3206 – 3013 (2004).
15. A. Lekatou, A. E. Karantzalis, A. Evangelou, et al., "Aluminium reinforced by WC and TiC nanoparticles (ex-situ) and aluminide particles (in-situ): Microstructure, wear and corrosion behavior," *Mater. Des.*, **65**, 1121 – 1135 (2015).
16. A. Mazahery and M. O. Shabani, "Influence of the hard coated B₄C particulates on wear resistance of Al–Cu alloys," *Composites: Part B*, **43**, 1302 – 1308 (2012).
17. P. Ravindran, K. Manisekar, R. Narayanasamy, and P. Narayanasamy, "Tribological behavior of powder metallurgy processed aluminium hybrid composites with the addition of graphite solid lubricant," *Ceram. Internat.*, **39**, 1169 – 1182 (2013).
18. M. V. Gorshenkov, S. D. Kaloshkin, V. V. Tcherdyntsev, et al., "Dry sliding friction of Al-based composites reinforced with various boron-containing particles," *J. Alloys Compd.*, **536**, S126 – S129 (2012).
19. N. Natarajan, S. Vijayarangan, and I. Rajendran, "Wear behaviour of A356/25SiCp aluminium matrix composites sliding against automobile friction material," *Wear*, **261**, 812 – 822 (2006).
20. A. Daoud, M. T. Abou El-Khair, and P. Rohatgi, "Wear and friction behavior of near eutectic Al–Si + ZrO₂ or WC particle composites," *Compos. Sci. Technol.*, **64**, 1029 – 1040 (2004).
21. C. S. Ramesh and R. Keshavamurthy, "Slurry erosive wear behavior of Ni–P coated Si₃N₄ reinforced Al6061 composites," *Mater. Des.*, **32**, 1833 – 1843 (2011).
22. P. Sharma, S. Sharma, and D. Khanduja, "Production and some properties of Si₃N₄ reinforced aluminium alloy composites," *J. Asian Ceram. Soc.*, **3**, 352 – 359 (2015).
23. Y. S. Kim, K. T. Kim, and S. J. Kim, "Sliding wear behavior of Al/SiC composites fabricated by thermal spray process against different counterparts," *Key Eng. Mater.*, **353 – 358**, 844 – 847 (2007).
24. K. Mizuuchi, K. Inoue, Y. Agari, et al., "Processing and thermal properties of Al/AlN composites in continuous solid–liquid co-existent state by spark plasma sintering," *Compos. : Part B*, **43**, 1557 – 1563 (2012).
25. Y. S. Kim and K. T. Kim, "Wear behavior of SiC reinforced metal matrix composites fabricated by thermal spray process," *Key Eng. Mater.*, **326 – 328**, 1845 – 1848 (2006).
26. M. J. Ghazali, W. M. Rainforth, and H. Jones, "The wear of wrought aluminium alloys under dry sliding conditions," *Tribology Int.*, **40**, 160 – 169 (2007).
27. I. L. Tangen, Y. Yu, T. Grande, et al., "Preparation and characterisation of aluminium nitride–silicon carbide composites," *Ceram. Internat.*, **30**, 931 – 938 (2004).
28. N. M. Kumar, S. S. Kumaran, and L. A. Kumaraswamidhas, "High temperature investigation on EDM process of Al 2618 alloy reinforced with Si₃N₄, AlN and ZrB₂ in-situ composites," *J. Alloys Compd.*, **663**, 755 – 758 (2016).
29. B. N. Pramila Bai, B. S. Ramasesh, and M. K. Surappa, "Dry sliding wear of A356–Al–SiC_p composites," *Wear*, **157**, 295 – 304 (1992).
30. S. Chaudhury, C. Sivaramakrishnan, and S. Panigrahi, "A new spray forming technique for the preparation of aluminium rutile (TiO₂) ex situ particle composite," *J. Mater. Proc. Technol.*, **145**, 385 – 390 (2004).
31. M. T. Abou El-Khair, "Microstructure characterization and tensile properties of squeeze-cast AlSiMg alloys," *Mater. Lett.*, **59**, 894 – 900 (2005).
32. A. B. Gurcan and T. N. Baker, "Wear behaviour of AA6061 aluminium alloy and its composites," *Wear* **188**, 185 – 191 (1995).
33. S. K. Sharma, B. V. M. Kumar, K. Y. Lim, et al., "Erosion behavior of SiC – WC composites," *Ceram. Internat.* **40**, 6829 – 6839 (2014).
34. W. Zhaohui, W. Xu-dong, Z. Yu-xin, and D. Wen-bo, "SiC nanoparticles reinforced magnesium matrix composites fabricated by ultrasonic method," *Trans. Nonferrous Met. Soc. China*, **20**, 1029 – 1032 (2010).
35. A. P. Shen Shaga, Ch. Sun, and Q. Jiang, "Lamellar-interpenetrated Al–Si–Mg/SiC composites fabricated by freeze casting and pressureless infiltration," *Mater. Sci. Eng. A*, **630**, 78 – 84 (2015).
36. L. Micele, G. Palombarini, S. Guicciardi, and L. Silvestroni, "Tribological behaviour and wear resistance of a SiC–MoSi₂ composite dry sliding against Al₂O₃," *Wear*, **268**, 368 – 375 (2010).
37. N. Mathan Kumar, S. Senthil Kumaran, and L. A. Kumaraswamidhas, "An investigation of mechanical properties and material removal rate, tool wear rate in EDM machining process of Al2618 alloy reinforced with Si₃N₄, AlN and ZrB₂ composites," *J. Alloys Compd.*, **650**, 318 – 327 (2015).
38. C. S. Ramesh, R. Keshavamurthy, S. Pramod, and P. G. Koppad, "Abrasive wear behavior of Ni–P coated Si₃N₄ reinforced Al6061 composites," *J. Mater. Process. Technol.*, **211**, 1423 – 1431 (2011).
39. X. Zi-yang, C. Guo-qin, W. Gao-hui, et al., "Effect of volume fraction on microstructure and mechanical properties of Si₃N₄/Al composites," *Trans. Nonferrous Met. Soc. China*, **21**, s285 – s289 (2011).

40. H. B. Michael Rajan, S. Ramabalan, I. Dinaharan, and S. J. Vijay, "Synthesis and characterization of in situ formed titanium diboride particulate reinforced AA7075 aluminum alloy cast composites," *Mater. Des.*, **44**, 438 – 445 (2013).
41. J. W. Kaczmar, K. Pietrzak, and W. Wlosinski, "The production and application of metal matrix composite materials," *J. Mater. Process. Technol.*, **106**, 58 – 67 (2000).
42. M. M. Schwartz, *Composite Materials. Volume II: Processing, Fabrication and Applications*, ASM International (1997).
43. M. T. Abou El-Khair, A. Daoud, and A. N. Abdel, "Effect of casting technology on the wear behaviour of A356 Al–Al₂O₃ or ZrO₂ composites," *4th Arab Cast Conference* (2002).
44. A. Daoud, M. T. Abou El-Khair, and A. N. Abdel Azim, "Microstructure and wear behavior of squeeze cast 7075 Al–Al₂O₃ particle composites," 14th International Offshore and Polar Engineering Conference (2004).
45. K. Mizuuchi, K. Inoue, Y. Agari, et al., "Thermal properties of diamond particle dispersed aluminum matrix composites fabricated in continuous solid–liquid co-existent state by SPS," *J. Jpn. Soc. Powder Metall.*, **56**, 438 – 443 (2009).
46. A. Eucken, "Heat transfer in ceramic refractory materials: calculation from thermal conductivities of constituents," *Fortch. Gebiete Ingenieurw. B. Forschungsheft*, **16**, 353 – 360 (1932).
47. T. Maiyajima and Y. Iwai, "Effects of reinforcements on sliding wear behavior of aluminum matrix composites," *Wear*, **255**, 606 – 616 (2003).
48. H. Zhang, M. W. Chen, K. T. Ramesh, et al., "Tensile behavior and dynamic failure of aluminum 6092/B₄C composites," *Mater. Sci. Engineer. A*, **433**, 70 – 82 (2006).
49. P. Cavaliere, E. Cerri, and P. Leo, "Effect of heat treatments on mechanical properties and damage evolution of thixoformed aluminium alloys," *Mater. Charact.*, **55**, 35 – 42 (2005).